TITLE

Subunit joining exposes nascent pre-40S rRNA for processing and quality control

AUTHORS

Jay Rai[1], Melissa D. Parker[2], Homa Ghalei[2,3], Matthew C. Johnson[1,4], Katrin Karbstein[2,5,6] and M. Elizabeth Stroupe[1,6]

[1] Department of Biological Science and the Institute of Molecular Biophysics, Florida State University, Tallahassee, Florida, 32306

[2] Department of Integrative Structural and Computational Biology, The Scripps Research Institute, Jupiter, Florida, 33458

[3] Present address: Department of Biochemistry, Emory University School of Medicine, Atlanta, Georgia

[4] Present address: Department of Biochemistry, University of Washington, Seattle, WA 98195

[5] HHMI Faculty Scholar

[6] To whom correspondence should be addressed: kkarbst@scripps.edu; mestroupe@bio.fsu.edu

RUNNING TITLE

Structure of an 80S-like ribosome assembly intermediate

Abstract

During their maturation, nascent 40S subunits enter a translation-like quality control cycle, where they are joined by mature 60S subunits to form 80S-like ribosomes. While these assembly intermediates are essential for maturation and quality control, how they form, and how their structure promotes maturation and quality control remains unknown. To address these questions, we solved the structure of an 80S-like ribosome assembly intermediate to an overall resolution of 3.4 Å. The structure, validated by biochemical data herein, resolves a large body of previously paradoxical data and illustrates how assembly and translation factors cooperate to promote the formation of an interface that lacks many mature subunit contacts but is stabilized by the universally conserved Dim1. The structure also shows how this interface leads to unfolding of the platform, which allows for temporal regulation of the ATPase Fap7 and the nuclease Nob1, thus linking quality-control and 40S maturation during ribosome assembly.

(Introduction)

Ribosome assembly is a highly regulated process, which begins with transcription, processing and folding of the rRNA in the nucleolus. Coupled to these co-transcriptional events is the binding of most ribosomal proteins. Largely assembled precursors are then exported into the cytoplasm, where they undergo final maturation, which, crucially, is coupled to quality control steps, to ensure that only correctly and fully-matured subunits are released into the translating pool[1,2]. For the small subunit, cytoplasmic quality control involves a translation-like cycle in which nascent 40S subunits are joined in an eIF5B-dependent manner by mature 60S subunits to produce 80S-like ribosomes[3,4]. These 80S-like ribosomes are hubs for quality control and maturation[5,6]. Despite the proliferation of structural information on very early nucleolar[7-9], as well as initial cytoplasmic 40S assembly intermediates[10-14], no structural information has been available for 80S-like ribosomes, despite their central role for quality control and maturation. Here, we use single-particle cryogenic electron microscopy (cryo-EM) to visualize the structure of 80S-like ribosomes that accumulate after depletion of the essential ATPase Fap7, a key player in quality control[6]. The structure is validated by biochemical data herein, as well as previous structural and biochemical data, and illuminates how 80S-like ribosomes harboring the key assembly factors Dim1 and Tsr1 form, despite their position that blocked joining in earlier assembly intermediates. Furthermore, the structure also suggests how the formation of 80S-like ribosomes enables rRNA maturation and quality control.

RESULTS AND DISCUSSION

To better understand how 40S ribosomes are matured and how this maturation is quality-controlled via structural and functional mimicry of translation events, we used single-particle cryo-electron microscopy (cryo-EM) to visualize the structure of the 80S-like ribosome that accumulates after depletion of the essential ATPase Fap7. These ribosome assembly intermediates were purified via a TAP-tag on the assembly factor (AF) Tsr1 (**Extended Data Figure S1a**). Importantly, previous biochemical data have already confirmed that these assembly intermediates are on pathway, as addition of recombinant Fap7 and ATP leads to the release of Dim1, and the formation of a hybrid-like state[6].

Initial three-dimensional alignment and classification identified two populations of particles. One was refined to a resolution of 3.6 Å, had features similar to mature 80S ribosomes (**Extended Data Figure S1b**), and was similar to a recently noted 80S pre-ribosome lacking assembly factors[13]. In this subclass of pre-ribosomes that lacked the AFs Tsr1, Dim1 and Pno1, the platform, beak, decoding helix, and bridge B3 are in their mature conformation and there is no density for a tRNA in any position (**Extended Data Figure S1c**). The other subclass had strong 60S density but weaker pre-40S density. Further refinement of the small or large subunit alone by masking out the density of the other subunit improved the clarity of the small subunit to an overall resolution of 3.7 Å and the large subunit to an overall resolution of 3.4 Å (**Extended Data Figure S1d)**. The small subunit remained anisotropic, with local resolutions ranging from ~3.4 Å at its core to ~10 Å at the interface and the platform (**Extended Data Figure S1e)**. Therefore, we performed local classification of the 60S subunit including the bridge between H69 and h24/Dim1 as well as at the platform, the results of which are shown in **Figure 1a-b** and described below. The details of this local classification are described in the methods.

Movements of the small subunit relative to the large subunit

The improvement in resolution when the pre-40S subunit was refined in isolation indicated that it is mobile relative to the large subunit. Subsequent multi-body analysis[15] indicated several independent motions of pre-40S relative to 60S. Most of these can be described by the first three Eigen vectors that correspond to three independent motions (**Extended Data Figure S2a**). 40S is mobile relative to 60S in mature ribosomes[15]; however, the motions that pre-40S undergoes in this intermediate are more extreme, because there are fewer subunit bridges formed in this assembly intermediate (see below), enabling a larger range of motion. Further, while in mature ribosomes the 40S head moves independently from the body[15], in 80S-like pre-ribosomes pre-40S moves as a rigid body, rotating both outward from 60S and parallel to the interface (**Extended Data Figure S2b**). The movement described by the first Eigenvector somewhat resembles that occurring during translocation, albeit more exaggerated. Importantly, the position of the pre-40S relative to the 60S subunit is consistent with our previous solution footprinting data, which showed that 80S-like ribosomes are in a classic-like state[6]. In fact, in the composite position of pre-40S relative to 60S, 80S-ribosomes appear to be hyper-classic (positioned away

from the rotated state by a 23° counter-clockwise rotation from the classic state, **Extended Data Figure S3**).

80S-like pre-ribosomes are joined via an immature interface

Overall, in 80S-like ribosomes, the pre-40S subunit is opened away from the 60S, creating space between the subunits and allowing for movement of the Tsr1 and Dim1 AFs relative to their position in isolated pre-40S ribosomes (**Figure 1a-c**). This allows for accommodation of Tsr1, Dim1 and h44, which is pulled out from the subunit interface in earlier pre-40S[11-14] and here as well (**Figure 1c)**. As a result, the subunit interface in 80S-like pre-ribosomes is formed by fewer intersubunit bridges than in mature 80S. Because the pre-40S subunit head is positioned far from the central protuberance of the already mature 60S, the B1a, b, and c bridges, which involve the 40S head, are not yet formed (**Figure 1d**). Similarly, the pre-40S is turned away from the 60S on the platform side and moved towards it on the beak side. As a consequence, bridge B7a cannot form because that side of the head is now too distant from the 60S (**Figure 1b, d)**. Further, the novel position of pre-40S relative to 60S accommodates the immature position of h44, which is shifted left, thus preventing formation of the bridges at the top of h44, including B3 and B5 (**Figure 1b, d**)[11,13]. In contrast, the eukaryote-specific bridges at the 40S foot are largely maintained, including eB8, eB10, eB11, eB12, and eB13 (**Figure b, d)**. In the case of a B5/B8-like bridge between h44 and L23 and a B6-like bridge between h44 and L24, the intersubunit connections are shifted due to the novel orientations of the two subunits but involve analogous interactions between the same structural elements (**Figure 1d and Extended Data Figure S4**).

The most surprising difference between this 80S-like assembly intermediate and mature 80S ribosomes is the change in the interaction of H69 from the large subunit with the small subunit. H69 is the target of RRF[16], which dissociates ribosomes, as well as some antibiotics[17-19], demonstrating its central role for the stability of 80S ribosomes. In mature 80S ribosomes, H69 forms an A-minor interaction with h44[20] to establish the B2a bridge (**Figure 1e**). In contrast, in 80S-like pre-ribosomes, H69 binds h24 (**Figure 1f**), which is substantially moved from its mature position (see below).

Tsr1 is repositioned towards the beak

In earlier 40S assembly intermediates, the AF Tsr1 binds parallel to h44, between the 40S body and beak, and interacting with another AF, Rio2[11-14] (**Figure 2** and **Extended Data Figure S5a**). In these earlier structures Tsr1's N-terminal α-helix is inserted behind h44, forcing h44 away from the body and inhibiting subunit joining by blocking the binding of eIF5B, the translation factor required for subunit joining[12,14,21]. In 80S-like pre-ribosomes, which have released Rio2, Tsr1 is no longer attached to the beak, moving via a rigid-body movement around a hinge at Ala63 within the helix that remains under h44, towards the tip of the beak and away from its position in isolated pre-40S (**Figure 2a-b, Extended Data Figure S5b, Supplemental Movie 1**). Interestingly, our previous dataset of earlier 40S assembly intermediates[12] contains a small population of molecules in which Tsr1 appears to be similarly rotated (**Extended Data Figure S6a**). Tsr1 in this low-resolution structure appears to have a disordered C-terminal domain either due to its mobility in isolated pre-40S or owing to the small particle number that contribute to the structure, but suggest that Tsr1's movement away from h44 and the beak is intrinsic to Tsr1 and the pre-40S subunit and not induced by eIF5B, but perhaps stabilized by it.

The intermediate herein accumulates after the activity and dissociation of eIF5B[4]. Thus, as expected based on previous biochemical data[4], eIF5B is not bound to this intermediate. Nevertheless, to gain insight into how eIF5B could interact with nascent 40S and 80S-like ribosomes, we docked eIF5B into this 80S-like pre-ribosome structure by superimposing the 60S subunits in our complex and the previously visualized mature 80S•eIF5B complex[22]. This analysis suggests that the postulated clashes between Tsr1 and eIF5B[21] are largely resolved in these 80S-like ribosomes. Importantly, they are resolved because of the opened position of pre-40S relative to 60S, which leaves the eIF5B binding site on the large subunit exposed, while allowing space for eIF5B behind Tsr1 at the subunit interface (**Figure 2c-d)**. Thus, the presence of Tsr1 promotes formation of this alternative subunit interface in 80S-like ribosomes, via three mechanisms: First, Tsr1 forces out h44, thereby sterically preventing the subunits from approaching each other more closely to form the subunit bridges in the head (**Figure 1a**); Second, Tsr1 stabilizes the interface due to its interaction with both pre-40S and 60S (**Extended Data Figure S6b)**; and third, Tsr1 blocks access of eIF5B to its typical binding site on 40S, preventing the formation of the B3 bridge (**Figure 2c-d**). Further, the relationship between eIF5B and the nascent 40S in this position suggests that eIF5B also contributes to the formation

of this immature interface because it lies across h44, just below the decoding site, where the B3 bridge forms in mature 80S ribosomes (**Figure 2c)**. The B3 bridge is a strong and early-forming bridge[23], so eIF5B binding at this position would block it from forming, thereby steering the subunits into the alternative conformation. In summary, the alternative subunit conformation allows for Tsr1 to remain bound while accommodating eIF5B, enabling eIF5B to promote formation of 80S-like pre-ribosomes.

rRNA folding and protein assembly to the nascent 40S subunit

Previous structures showed that earlier pre-40S subunits lack Rps10, Rps26 and Asc1[4,11-14] and the tip of h31 remains unfolded[11,13]. In this intermediate, clear density for Asc1 and Rps10 is apparent at their mature position in the head (**Extended Data Figure S7)**, indicating that these proteins are recruited prior to Fap7 activity, as expected based on our previous biochemical analyses[4]. Furthermore, the tip of h31 is clearly visible (**Extended Data Figure S8**). This coincides with the beak moving forward to its mature position while the overall head configuration straightens (**Extended Data Figure S9**), movements that occur where the 40S head joins the body and near the Tsr1 and Rio2 binding sites. Specifically, in earlier pre-40S intermediates Tsr1 binds immediately adjacent to the last ordered nucleotide in h31 and Rio2 is bound adjacent to where the helix is located in mature 40S subunits[11-14]. We suggest that these changes arise from dissociation of Rio2 and detachment of Tsr1 from the head in 80S-like pre-ribosomes, indicating roles for these two maturation events in promoting the folding of h31.

Dim1 is repositioned with h24

Dim1's position in pre-40S subunits inhibits subunit joining by sterically blocking the approach of H69 from the 60S subunit[11-14]. As described above, H69 remains the main connection between the subunits in 80S-like ribosomes. Thus, in contrast to Tsr1, the alternative subunit interface in 80S-like ribosomes does not alleviate the steric block from Dim1. While even our initial structures identified Dim1 in its remodeled position (**Figure 3a)**, its structure was further clarified by extensive localized classification and refinement as described in the methods. Even though the resolution remains relatively low, this analysis shows that to allow for H69 binding, Dim1 moves with h24 by maintaining its interactions with the lower part of the helix and forming new contacts near its top (**Figure 3b-c, Supplemental Movie 2**). This rotation of h24

away from the platform repositions Dim1 above H69, alleviating the steric conflict. To validate the low-resolution position of Dim1 and probe the importance of the newly established contacts between Dim1 and h24 in subunit joining, we created a variant Dim1-FRK (F231L, R233E, K234E, orange in **Figure 3**) and tested its effect on yeast growth and subunit joining. In 80S-like pre-ribosomes these residues make interactions with the repositioned h24 (**Figure 3a-b, d**). These variants were tested in a galactose-inducible, glucose-repressible yeast strain, so that plasmid-encoded wild type or mutant Dim1 was the only Dim1 source. Dim1_FRK does not support growth, showing the importance of these residues for ribosome assembly. To test more directly if the residues are important for subunit joining or have a function in an earlier stage of ribosome assembly, we co-depleted Fap7 in a second yeast strain. When subunit joining is possible, depletion of Fap7 leads to the accumulation of pre-40S ribosomes in 80S-like complexes, as indicated by the co-sedimentation of pre-18S rRNA and 25S rRNA in 80S-sized fractions[4]. Importantly, yeast with wild type Dim1, but not Dim1-FRK, form 80S-like ribosomes upon Fap7 depletion or inactivation, as indicated by the shift of 20S pre-rRNA from the 80S to the 40S fraction (**Figure 3e)**, demonstrating the importance of the observed Dim1-h24 interaction in subunit joining. We have previously shown that the weakly binding Dim1_EKR variant allows for subunit joining, but is then released Fap7-independently. Thus, subunit joining is not generally affected when Dim1•rRNA interactions are weakened, and the phenotype from the Dim1-FRK mutants specific. Thus, the interpretation of this relatively low-resolution part of the structure is validated independently through biochemical experiments. Further, as we will describe below, the position of Dim1 is additionally validated by published biochemical experiments that demonstrate an interaction between Dim1, Fap7 and Rps14[6].

The platform is substantially unfolded

In addition to the remodeled H69 bridge, extensive differences between earlier pre-40S subunits and this complex are also observed at the platform, where a rigid body motion opens the platform towards the large subunit (**Figure 4a-b**). Importantly, the other major subclass of 80S ribosomes we observe in our preparations has a canonical platform (**Figure S1c)**, ruling out artifacts during sample purification or preparation for cryo-EM as causative for the platform rearrangements described below. Furthermore, no preferential orientation in the molecules were

observed, as expected if a subpopulation of molecules were interacting preferentially with the slide or air-water interface thus unfolding the platform.

Local classification reveals three dominant classes with varying densities near to the Rps1 and Rps14 binding sites (**Extended Data Figure S10)**. One subclass has a horseshoe-shaped density at about 10 Å resolution, that corresponds well to the shape of the Rps1•14 dimer (**Figure 4a and Extended Data Figure S10a)**. A second subclass shows only the density that corresponds to Rps14, supporting our assignment of the Rps1•Rps14 dimer in subclass 1 (**Extended Data Figure S10b)**. The third subclass is of lower resolution but whose platform accommodates Rps1•Rps14 and two KH domains of Pno1, consistent with the interaction of Pno1 with Rps1 and Rps14 in earlier pre-40S subunits[11,13] (**Extended Data Figure S10c).** This local heterogeneity suggests that the platform is highly mobile in this intermediate, with partial occupancy of these ribosomal proteins, consistent with previous biochemical data[4]. The partial loss of Rps14 and Rps1, which bind h23/24 and the repositioning of Dim1 from h45 to h24, are likely responsible for the disorder in these now mobile RNA helices[24,25].

Importantly, this opened platform structure explains multiple puzzling and paradoxical previous observations as described below. For example, biochemical and mass spectrometry analyses have demonstrated the partial loss of Rps1 and Rps14 in 80S-like pre-ribosomes *in vivo*[4], thereby essentially predicting this structure. Moreover, this structure illuminates how Fap7 is recruited and functions in release of Dim1 (**Figure 4c)**: While a previous crystal structure had revealed the structure of the Fap7•Rps14 complex[26], this structure had demonstrated that the site where Rps14 interacts with Fap7 was identical to the site where Rps14 binds h23[26]. Because Rps14 recruits Fap7[26-29], but binds h23 early during assembly[7-9], how Fap7 was recruited remained puzzling. The structure of this intermediate (accumulated in the absence of Fap7) shows how it is poised for Fap7 binding, as h23 is mobilized (or unfolded), thereby freeing up Rps14 to recruit Fap7. Importantly, docking the Fap7•Rps14 crystal structure[26] onto Rps14 in the 80S-like structure, not only accommodates Fap7, but places it in contact with Dim1 (**Figure 4d**), consistent with their direct binding in solution[6]. Thus, this relatively low-resolution part of the structure is validated by our own mutagenesis (**Figure 3d-e)**, previous crystal structures of Fap7•Rps14[26], protein-

protein interactions between Fap7 and Dim1[6], and mass-spectrometry analyses of 80S-like ribosomes[4].

Pno1 is bound in our intermediate (**Extended Data Figure S1a)**, but density for it is not obvious in the major platform subclass (**Figure 4a**). Assuming the interactions between Rps1, Rps14 and Pno1 observed in previous 40S assembly intermediates[11,13] were maintained, we docked Rps1•Rps14• Pno1•Nob1 from these assembly intermediates (PBD ID 6G18[10]) onto the 80S-like structure, where Pno1 then falls into the middle of the horse-shoe-like density for Rps1 and Rps14 (**Figure 4e)**. Importantly, one of the platform subclasses has density in that region, in addition to Rps1 and Rps14, albeit at low resolution (**Extended Data Figure S10c)**, supporting this placement for Pno1.

We next asked where this superimposition placed Nob1. In a structure of an earlier human 40S assembly intermediate, the Nob1 active site is positioned 30 Å and 90° away from the 3' end of the pre-rRNA (**Figure 4f,**[10]), suggesting that the position of Nob1 in this intermediate rendered it inactive. Thus, for Nob1 to mature the pre-18S rRNA, some reorganization of the platform would be necessary. Intriguingly, the outward movement of the platform in the 80S-like intermediate shifts the Rps1•Rps14•Pno1 complex, from where it is in earlier pre-40S subunits (**Figure 4a-b, e)**. Assuming the contacts between Nob1 and Pno1 are maintained, this repositioning moves Nob1 so that it is placed directly over the 3' end of the rRNA (**Figure 4f-g**). Importantly, this position is supported by crosslinks between Nob1 and U1054/1055 of 18S rRNA[30], which are hard to reconcile with the position of Nob1 in pre-40S[13]. Thus, the opening of the platform, promoted by the interaction of h24 with H69 of the 60S subunit, also repositions the Nob1•Pno1 complex to bring the Nob1 active site close to its rRNA substrate. This observation explains previous data suggesting that Nob1-dependent cleavage occurs in 80S-like ribosomes, but not earlier intermediates[5]. Thus, by repositioning and mobilization of the rRNA, Rps1 and Rps14, the opened structure of the platform in 80S-like ribosomes illustrates and explains the temporal regulation of Fap7 recruitment and Nob1 activation.

In summary, the structure of 80S-like pre-ribosomes presented here shows that the AFs Dim1 and Tsr1 are repositioned relative to their positions on earlier pre-40S, allowing for joining of the

60S subunit via an open and immature interface. Docking of eIF5B into the structure indicates how the AF Tsr1 and the translation factor eIF5B cooperate to promote the formation of this subunit interface, which accommodates both proteins at the opened GTPase-binding site, while maintaining the deformed conformation of h44. Furthermore, the structure also demonstrates a remodeled interface, largely dependent upon an interaction between H69 and h24, which replaces bridge B2a, and is stabilized by Dim1. To form this interface h24 must reposition, thereby opening the platform, which allows for recruitment of Fap7, and subsequent proofreading of the nascent 40S[6], and regulation of the Nob1 nuclease by repositioning of the Nob1•Pno1 complex. This structure, validated by genetic and biochemical data herein, as well as previous biochemical[6], mass spectrometry[4] and crystallographic[26] data, thereby explains how the formation of 80S-like ribosomes is required for proofreading and quality control of 40S ribosome maturation.

Online METHODS

Yeast strains and cloning: The Gal::Fap7;Gal::Dim1 and Gal::Fap7;Tsr1TAP yeast strains were produced using PCR-based recombination[31], and confirmed by PCR and western blotting. The Dim1-F231L, R233E, K234E (Dim1_FRK) mutations were introduced into pRS416TEF containing Dim1 by site-directed mutagenesis and confirmed by sequencing.

Sucrose density gradient analysis: Sucrose gradient fractionations of whole cell lysates, followed by Northern blot analysis, were performed as described previously[4]. To calculate the amount of 20S rRNA in the 80S-like fraction, the signal in the 40S fraction (fractions 3-4) and the 80S fraction (fractions 6-7) were quantified and the 80S signal was then divided by the sum of the 80S and 40S signal.

Antibodies: Antibodies against soluble recombinant Dim1 and Tsr1 were raised in rabbits by Josman LLP, and HRP-conjugated anti-rabbit secondary antibody was obtained from Rockland Immunochemicals.

Sample Purification and Preparation: Fap7 was depleted by growth in YPD for 16 hours. 2.5 mL of lysis buffer (30 mM HEPES-KOH pH 6.8, 100 mM NaCl, 6 mM $MgCl_2$, RNasin, PMSF, Benzamidine, EDTA – free protease inhibitor tablet (Santa Cruz Biotechnology, Dallas, TX, USA), Leupeptin, Pepstatin, and Aprotinin was added to 4 g of lysed frozen cell powder. The cell powder was mixed with 2 mL of Zircona silica beads (Millipore-Sigma, St. Louis, MO, USA) and vortexed 20 sec for homogenization. The frozen cell lysate thawed at 4 ˚C on a rocker. Thawed cell lysate was cleared via two centrifugations at 4˚C: first, at 3,000 x g for five min and second, at 10,000 x g for 10 min. The cleared supernatant was incubated with 250 µL of pre-equilibrated IgG beads (GE Healthcare, Little Chalfonte, UK) at 4˚C for 1.5 h with gentle

rotation. After incubation, the flow through was discarded and beads were washed three times with buffer A (30 mM HEPES-KOH pH 6.8, 100 mM NaCl, 6 mM $MgCl_2$, 0.075% NP-40, PMSF, Benzamidine) followed by an additional wash buffer B (30 mM HEPES-KOH pH 6.8, 100 mM NaCl, 6 mM $MgCl_2$, PMSF, Benzamidine). Washed beads were incubated with 250 µL TEV cleavage buffer (30 mM HEPES-KOH pH 6.8, 100 mM NaCl, 6 mM $MgCl_2$, PMSF, Benzamidine, 1 mM DTT and 0.5 mM EDTA) supplemented with 2.5 µL AcTEV protease (Invitrogen, Carlsbad, CA, USA) at 16˚C for two hours with gentle shaking. After incubation, flow through was collected. The concentration and quality of eluate was determined spectrophotometrically using a Nanodrop 1000 (Thermo Scientific, Waltham, MA, USA). 3 µL of eluate (72 nM) was applied to a plasma-treated UltraAuFoil 1.2/1.3 grid (Quantifoil, Großlöbichau, Germany). The grids were hand blotted for 3 sec from the backside of the grid before being plunged into liquefied ethane.

Microscopy and Refinement: Images were acquired on an FEI Titan Krios transmission electron microscope operated at 300 kV equipped with a DE64 (Direct Electron, San Diego, CA, USA) directed by the automated hole finder in Leginon (**Extended Data Tables 1 and 2**)[32]. Images were recorded in "movie mode" at a range of -1.3 to -2.5 µm defocus. A total of 25 $e^-/Å^2$ dose was spread over 42 frames at a nominal magnification of 59,000x, yielding a pixel size of 1.24 Å/pixel at the specimen level. The images that showed signs of astigmatism, poor ice, drift, empty holes or bad sample quality were discarded. In total, 4,193 micrographs were selected for frame alignment and dose compensation with the MotionCorr algorithm[33]. Initial CTF parameters were estimated using Gctf[34]. A total of 146,641 particles were selected by the auto-picking algorithm implemented and further processed in Relion-3.0, with per-particle CTF estimation and correction and beam-tilt correction[35]. 3D classification and 3D autorefine revealed 55,949 particles whose 60S and 40S subunits were at an orientation like mature 80S (empty pre-ribosome), as was seen before[13]. 90,692 particles had strong 60S density but diffuse 40S density (80S-like pre-ribosome). These structures were independently subjected to refinement using Relion-3's "autorefine" function. The empty pre-ribosome structure was refined to 3.6 Å resolution (Extended data Figures 1b-c). The 80S-like pre-ribosome structure (parent structure) was refined to 3.4 Å resolution, but with significant anisotropy in the pre-40S subunit. To better resolve the individual subunits, the 80S-like pre-ribosome structure was further refined either with a 3D custom mask on the 40S subunit or with a mask on the 60S subunit, yielding a structure of pre-40S at 3.7 Å-resolution and a structure of 60S at 3.4 Å resolution (Extended data Figure 1). To understand the nature of the anisotropy in the 80S-like pre-ribosome, the parent structure was further refined with the multi-body approach implemented in Relion-3 using two masks. A mask on 60S that included the bridge density was used as the first body and a 3D mask on pre-40S as second body with an 11 Å overlap. To further define the central density that bridges the two subunits, we performed local classification with a spherical mask that included H69 from 60S and the space where the now unfolded h45 is located in pre-40S. A dominant subclass emerged that, after further autorefinement in Relion3.0, revealed the position of Dim1 at the central bridging density still bound to the repositioned h24. Although the resolution of Dim1 remains relatively low (~10 Å), the density has the size, and shape of Dim1, and SDS-PAGE analysis demonstrates the presence of Dim1 in the complex. Furthermore, as described in detail in the results, the interactions between Dim1 and h24 are largely preserved in this structure and the previous pre-40S structures. H69 also has a resolution of ~10 Å and the contours of the major and minor grooves of the hairpin are clearly visible without any localized

classification. Finally, the repositioned h24 has a resolution of ~10 Å and the twist of the helix is also visible without any localized classification. Despite being at lower resolution than the core structure, these key central elements are clearly identifiable within the limits of the 10 Å resolution because of the distinct helical contours of the RNA helices and the two-domain construction of Dim1.

To understand the remaining anisotropy in the pre-40S subunit, we independently performed local classification of the pre-40S subunit with a spherical mask at the platform. The resulting structures were independently refined and yielded three major subclasses (**Figure S10)**. Two of these contain Rps1 and Rps14 in the presence and absence of a third protein, likely Pno1. A third class has only Rps14. These proteins were identified based on their location in mature ribosomes, and their size and shape, which matches that of these ribosomal proteins. Further confidence in the assignment as two independent proteins derives from the presence of only part of the density in subclass 2**.** Tentative assignment of the remaining density as Pno1 is supported by the binding of Pno1 next to Rps1 and Rps14 in mature 40S and earlier pre-40S ribosomes.

Model building

Pre-40S and 60S were independently modeled from the rotated, mature 80D ribosome (PDB ID 3J77 [22,36] First, subunits were rigid-body rotated into either half of the map to assess their relative orientation at the newly formed interface. 60S fit well with a few minor adjustments to Rpl19, H69, and the L1 stalk. For Rpl19, the alpha helical tail was manually fit into the newly-formed bridge in Coot [37]. The L1 stalk was rotated as a rigid body to fit the density. Then, the density was segmented from the main map with the "segmentation" tool in Chimera [38]. The coordinates for the L1 stalk were isolated from the remainder of the model and then rigid body fit into the density with the "fit in map" tool in Chimera, then re-joined to the main model manually. H69 was manually rotated in Coot to match the curve of the bridge density. The chain for Rlp41 was manually removed.

Pre-40S also required some adjustments to h24, the head, and Tsr1. No density was apparent for h23, Rps1, Rps26, or Rps14 in the consensus map so they were removed from the model. In Coot, h24 was rotated as a rigid body with minimal changes to match the contours of the remodeled bridge. The head density was segmented from the body from the main map with the "segmentation" tool in Chimera. The coordinates for the head rRNA and r-proteins were isolated from the remainder of the model and then rigid body fit into the density with the "fit in map" tool in Chimera, then re-joined to the main model manually. Tsr1 from the pre-40S ribosome (PDB ID 6FAI[13]) was rigid-body fit into the density joining the head to the body. Human Dim1 from PDB ID 6G18[10] was initially placed into the bi-lobed density at the main subunit bridge by docking it into the Dim1 density in the pre-40S ribosome map containing Dim1 (EMD-4218[13]) on its h24 binding site and then repositioning with h24 into the new h24 position so Dim1 filled the bi-lobed density. Then, the N- and C-terminal domains were adjusted as independent rigid bodies to match the contours of the two lobes. The linker was rebuilt to match the density in Coot[37]. Each model was then independently subjected to real space refinement against the best 60S or pre-40S map using the Phenix.real.space.refine algorithm[39]. The resulting pre-40S model had 89.7% amino acids in favored Ramachandran Plot regions and 0.2% in the outlier region. The overall Clashscore was 13.0%. The resulting 60S model had 85.9% amino acids in favored Ramachandran Plot regions and 0.2% in the outlier region. The overall Clashscore was 27.9%.

Despite using masks that overlapped by about 10 Å, the interface is less well-defined than the core regions of the individual subunits. Local classification and refinement in Relion 3.0 after masking out pre-40S, but including the bridge from 60S, revealed improved density for the bridge. Further local resolution-dependent low-pass filtering in Relion 3.0 reveals the contours for H69 from 60S and a double-stranded RNA helix that fits well in length to a remodeled h24 from pre-40S. The dimensions of a bimodal density between h24 and the P-stalk from 60S match the expected shape of the two-lobed Dim1, however the secondary structure elements were at insufficient resolution to model the structure. Separate local classification, refinement, and local resolution-dependent low-pass filtering of the pre-40S platform in Relion 3.0 revealed four majority classes with differing densities corresponding to Rps1, Rps14, and Pno1.

All structure figures were made in Chimera[38] and assembled in Photoshop (Adobe, San Jose, CA) without additional modification.

REFERENCES

1 Bassler, J. & Hurt, E. Eurokaryotic Ribosome Assembly. *Annu Rev Biochem*, doi:10.1146/annurev-biochem-013118-110817 (2018).

2 Klinge, S. & Woolford, J. L., Jr. Ribosome assembly coming into focus. *Nat Rev Mol Cell Biol*, doi:10.1038/s41580-018-0078-y (2018).

3 Lebaron, S. *et al.* Proofreading of pre-40S ribosome maturation by a translation initiation factor and 60S subunits. *Nat Struct Mol Biol* **19**, 744-753, doi:10.1038/nsmb.2308 (2012).

4 Strunk, B. S., Novak, M. N., Young, C. L. and Karbstein, K. A Translation-Like Cycle is a Quality Control Checkpoint for Maturing 40S Ribosome Subunits. *Cell* **150**, 111-121 (2012).

5 Garcia-Gomez, J. J. *et al.* Final pre-40S maturation depends on the functional integrity of the 60S subunit ribosomal protein L3. *PLoS Genet* **10**, e1004205, doi:10.1371/journal.pgen.1004205 (2014).

6 Ghalei, H. *et al.* The ATPase Fap7 Tests the Ability to Carry Out Translocation-like Conformational Changes and Releases Dim1 during 40S Ribosome Maturation. *Molecular cell* **67**, 990-1000 e1003, doi:10.1016/j.molcel.2017.08.007 (2017).

7 Barandun, J. *et al.* The complete structure of the small-subunit processome. *Nat Struct Mol Biol* **24**, 944-953, doi:10.1038/nsmb.3472 (2017).

8 Cheng, J., Kellner, N., Berninghausen, O., Hurt, E. & Beckmann, R. 3.2-A-resolution structure of the 90S preribosome before A1 pre-rRNA cleavage. *Nat Struct Mol Biol* **24**, 954-964, doi:10.1038/nsmb.3476 (2017).

9 Sun, Q. *et al.* Molecular architecture of the 90S small subunit pre-ribosome. *Elife* **6**, doi:10.7554/eLife.22086 (2017).

10 Ameismeier, M., Cheng, J., Berninghausen, O. & Beckmann, R. Visualizing late states of human 40S ribosomal subunit maturation. *Nature* **558**, 249-253, doi:10.1038/s41586-018-0193-0 (2018).

11 Heuer, A. *et al.* Cryo-EM structure of a late pre-40S ribosomal subunit from Saccharomyces cerevisiae. *Elife* **6**, doi:10.7554/eLife.30189 (2017).

12 Johnson, M. C., Ghalei, H., Doxtader, K. A., Karbstein, K. & Stroupe, M. E. Structural Heterogeneity in Pre-40S Ribosomes. *Structure* **25**, 329-340, doi:10.1016/j.str.2016.12.011 (2017).
13 Scaiola, A. *et al.* Structure of a eukaryotic cytoplasmic pre-40S ribosomal subunit. *Embo J* **37**, doi:10.15252/embj.201798499 (2018).
14 Strunk, B. S. *et al.* Ribosome assembly factors prevent premature translation initiation by 40S assembly intermediates. *Science* **333**, 1449-1453, doi:10.1126/science.1208245 (2011).
15 Nakane, T., Kimanius, D., Lindahl, E. & Scheres, S. H. Characterisation of molecular motions in cryo-EM single-particle data by multi-body refinement in RELION. *Elife* **7**, doi:10.7554/eLife.36861 (2018).
16 Pai, R. D. *et al.* Structural Insights into ribosome recycling factor interactions with the 70S ribosome. *Journal of molecular biology* **376**, 1334-1347, doi:10.1016/j.jmb.2007.12.048 (2008).
17 Borovinskaya, M. A. *et al.* Structural basis for aminoglycoside inhibition of bacterial ribosome recycling. *Nat Struct Mol Biol* **14**, 727-732, doi:10.1038/nsmb1271 (2007).
18 Prokhorova, I. *et al.* Aminoglycoside interactions and impacts on the eukaryotic ribosome. *Proc Natl Acad Sci U S A* **114**, E10899-E10908, doi:10.1073/pnas.1715501114 (2017).
19 Wang, L. *et al.* Allosteric control of the ribosome by small-molecule antibiotics. *Nat Struct Mol Biol* **19**, 957-963, doi:10.1038/nsmb.2360 (2012).
20 Ben-Shem, A. *et al.* The structure of the eukaryotic ribosome at 3.0 A resolution. *Science* **334**, 1524-1529, doi:10.1126/science.1212642 (2011).
21 McCaughan, U. M. *et al.* Pre-40S ribosome biogenesis factor Tsr1 is an inactive structural mimic of translational GTPases. *Nature communications* **7**, 11789, doi:10.1038/ncomms11789 (2016).
22 Fernandez, I. S. *et al.* Molecular architecture of a eukaryotic translational initiation complex. *Science* **342**, 1240585, doi:10.1126/science.1240585 (2013).
23 Shaikh, T. R. *et al.* Initial bridges between two ribosomal subunits are formed within 9.4 milliseconds, as studied by time-resolved cryo-EM. *Proc Natl Acad Sci U S A* **111**, 9822-9827, doi:10.1073/pnas.1406744111 (2014).
24 Davis, J. H. *et al.* Modular Assembly of the Bacterial Large Ribosomal Subunit. *Cell* **167**, 1610-1622 e1615, doi:10.1016/j.cell.2016.11.020 (2016).
25 Mulder, A. M. *et al.* Visualizing ribosome biogenesis: parallel assembly pathways for the 30S subunit. *Science* **330**, 673-677, doi:330/6004/673 [pii]
10.1126/science.1193220 (2010).
26 Loc'h, J. *et al.* RNA mimicry by the fap7 adenylate kinase in ribosome biogenesis. *PLoS Biol* **12**, e1001860, doi:10.1371/journal.pbio.1001860 (2014).
27 Granneman, S., Nandineni, M. R. & Baserga, S. J. The putative NTPase Fap7 mediates cytoplasmic 20S pre-rRNA processing through a direct interaction with Rps14. *Mol. Cell Biol.* **25**, 10352-10364 (2005).
28 Jakovljevic, J. *et al.* The carboxy-terminal extension of yeast ribosomal protein S14 is necessary for maturation of 43S preribosomes. *Mol. Cell* **14**, 331-342 (2004).

29 Hellmich, U. A. *et al.* Essential ribosome assembly factor Fap7 regulates a hierarchy of RNA-protein interactions during small ribosomal subunit biogenesis. *Proc Natl Acad Sci U S A* **110**, 15253-15258, doi:10.1073/pnas.1306389110 (2013).
30 Turowski, T. W. *et al.* Rio1 mediates ATP-dependent final maturation of 40S ribosomal subunits. *Nucleic acids research* **42**, 12189-12199, doi:10.1093/nar/gku878 (2014).
31 Longtine, M. S. *et al.* Additional modules for versatile and economical PCR-based gene deletion and modification in Saccharomyces cerevisiae. *Yeast* **14**, 953-961 (1998).
32 Carragher, B. *et al.* Leginon: an automated system for acquisition of images from vitreous ice specimens. *J Struct Biol* **132**, 33-45, doi:10.1006/jsbi.2000.4314 (2000).
33 Li, X. *et al.* Electron counting and beam-induced motion correction enable near-atomic-resolution single-particle cryo-EM. *Nature methods* **10**, 584-590, doi:10.1038/nmeth.2472 (2013).
34 Zhang, K. Gctf: Real-time CTF determination and correction. *J Struct Biol* **193**, 1-12, doi:10.1016/j.jsb.2015.11.003 (2016).
35 Zivanov, J. *et al.* New tools for automated high-resolution cryo-EM structure determination in RELION-3. *Elife* **7**, doi:10.7554/eLife.42166 (2018).
36 Svidritskiy, E., Brilot, A. F., Koh, C. S., Grigorieff, N. & Korostelev, A. A. Structures of yeast 80S ribosome-tRNA complexes in the rotated and nonrotated conformations. *Structure* **22**, 1210-1218, doi:10.1016/j.str.2014.06.003 (2014).
37 Emsley, P., Lohkamp, B., Scott, W. G. & Cowtan, K. Features and development of Coot. *Acta Crystallogr D Biol Crystallogr* **66**, 486-501, doi:10.1107/S0907444910007493 (2010).
38 Pettersen, E. F. *et al.* UCSF Chimera--a visualization system for exploratory research and analysis. *J Comput Chem* **25**, 1605-1612, doi:10.1002/jcc.20084 (2004).
39 Adams, P. D. *et al.* PHENIX: a comprehensive Python-based system for macromolecular structure solution. *Acta Crystallogr D Biol Crystallogr* **66**, 213-221, doi:10.1107/S0907444909052925 (2010).
40 Ghalei, H. *et al.* Hrr25/CK1δ-directed release of Ltv1 from pre-40S ribosomes is necessary for ribosome assembly and cell growth. *Journal of Cell Biology* **208**, 745-759 (2015).

ACKNOWLEDGEMENTS

This work was supported by NIH grants R01-GM117093 and R01-GM086451, and HHMI Faculty Scholar grant 55108536 to K.K.. The authors acknowledge the use of instruments at the Biological Science Imaging Resource supported by Florida State University and NIH grants S10 RR025080, S10 OD018142, and U24 GM116788. H.G. was supported in part by a PGA National Women's Cancer Awareness Postdoctoral Fellowship. We wish to thank members of the Karbstein lab for comments on the manuscript, and Drs. Scott Stagg and Kenneth Taylor for useful discussions. J.R. and H.G. prepared samples; J.R. and M.E.S. carried out structure

reconstruction; M.D.P. carried out yeast analyses; M. C. J. performed cryo-EM analysis of pre-40S; K.K. and M.E.S. conceived of the experiments and wrote the paper.

COMPETING INTERESTS

The authors have no competing interests.

MATERIALS AND CORRESPONDENCE

Correspondence requests should be addressed to: M.E. Stroupe, mestroupe@bio.fsu.edu
Materials requests should be addressed to: K. Karbstein, kkarbst@scripps.edu

FIGURES AND LEGENDS

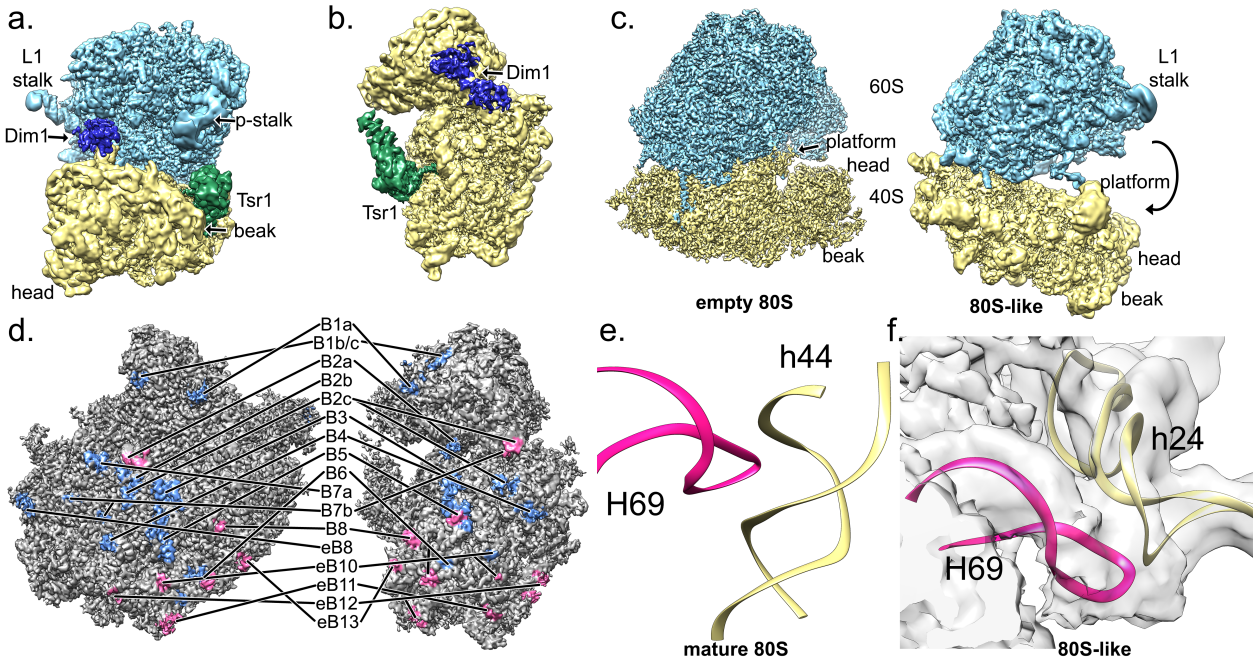

Figure 1: 80S-like ribosomes join via an immature interface. a. Overall structure of 80S-like ribosomes. 60S is light blue, pre-40S is yellow, Dim1 is dark blue, and Tsr1 is green. **b.** The pre-40S interface has only Tsr1 (green) and Dim1 (blue) bound. **c.** In the 80S-like pre-ribosome the space between the subunits is expanded. **d.** The bridges between 60S and the pre-40S head and central region of the body are largely not formed (blue patches) while those with the pre-40S foot remain intact or modestly reorganized (pink). **e.** In mature ribosomes, helix 69 from the 60S subunit (H69, pink) binds helix 44 from the pre-40S subunit (h44, cyan, model from PDB ID 3J77[36]). **f.** 80S-like ribosomes join through a novel bridge B2a/c where H69 (pink) joins a repositioned h24 (cyan).

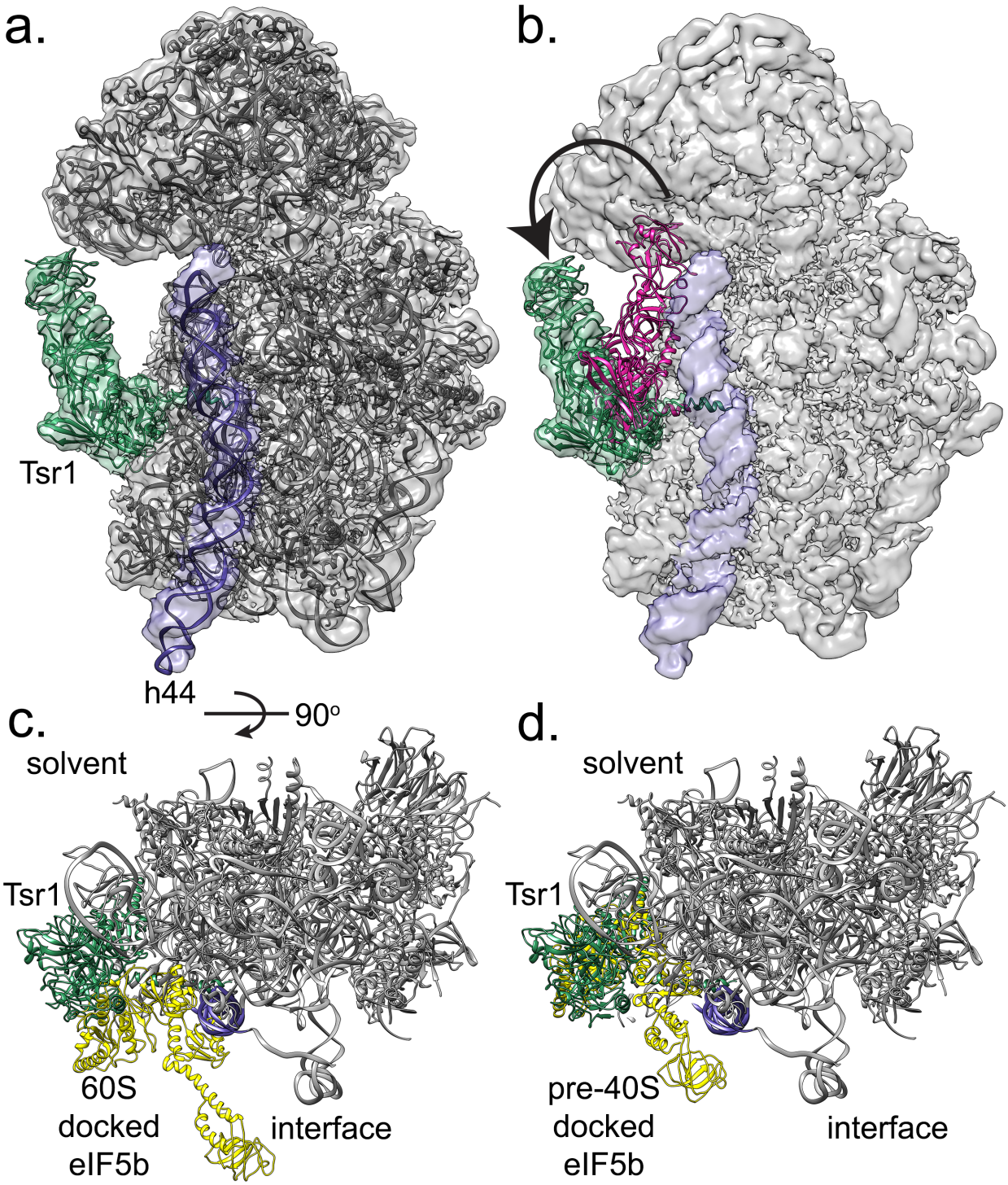

Figure 2: Tsr1 is repositioned to the beak. a. Tsr1 (green) in 80S-like ribosomes. **b.** The position of Tsr1 in 80S-like ribosomes (green) is substantially different from the position previously identified in an earlier cytoplasmic pre-40S intermediate (pink) (Model from EMD-8349[12]). **c.** The opened pre-40S and 60S interface leaves space for eIF5B (yellow) across h44, blocking the early-forming B3 bridge. Model was obtained by superimposition of the 60S subunits from the 80S-like pre-ribosome structure here and the eIF5B-bound mature 80S

ribosome (PDB ID 4V8Z[22]). **d.** If subunits were joining in the canonical mature 80S-structure, Tsr1 binding would block eIF5B recruitment. Model was obtained by superimposition of the 40S subunits from the 80S-like pre-ribosome structure here and the eIF5B-bound mature 80S ribosome (PDB ID 4V8Z[22]).

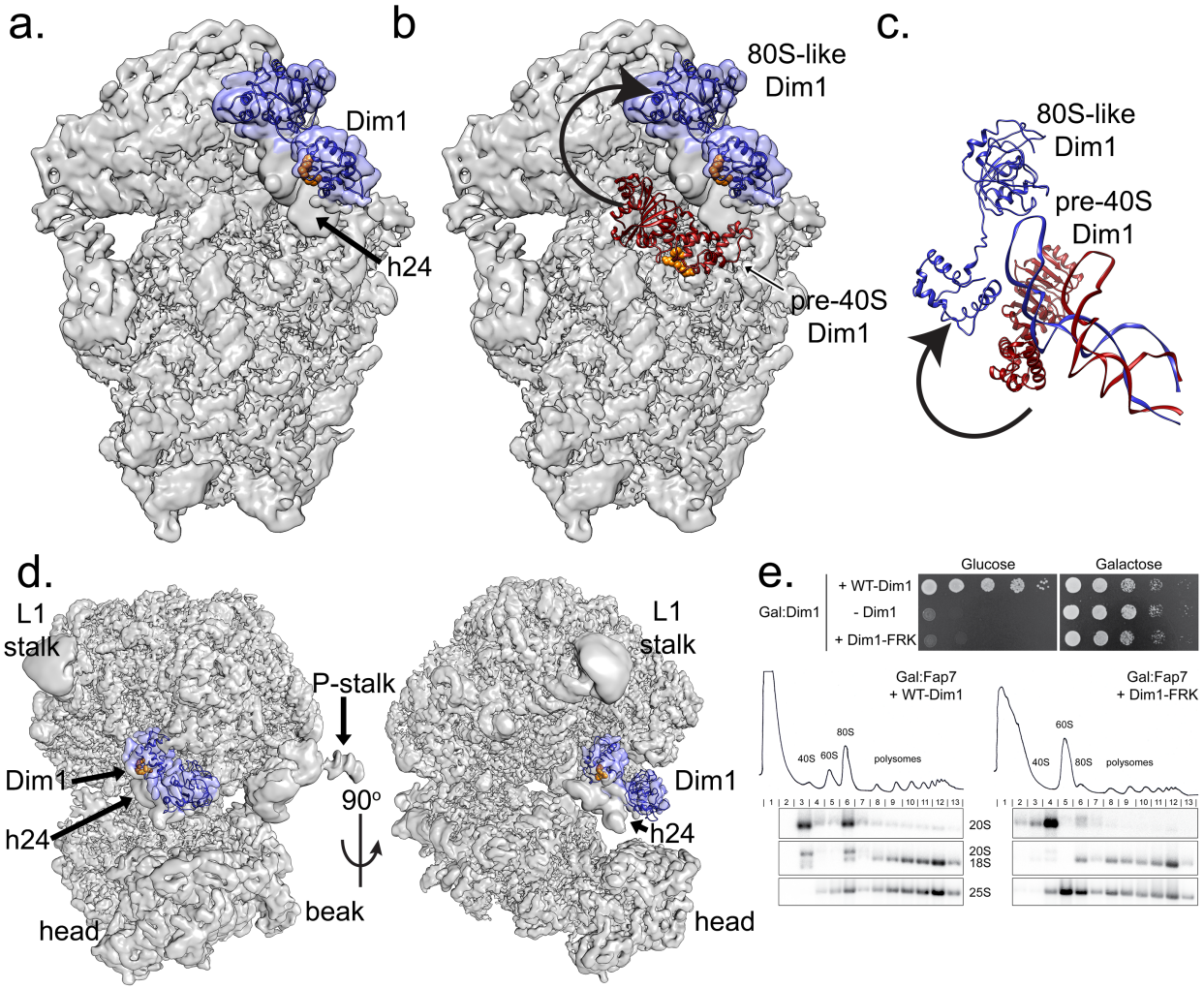

Figure 3: Dim1 binds h24 at the 80S-like pre-ribosome interface. a. Local classification followed by refinement and local B-factor sharpening in Relion 3.0 revealed a bi-lobed density at the 60S-pre-40S interface that matches the Dim1 structure (blue). Phe231, Arg233, and Lys234 (Dim1-FRK) are shown in orange. **b.** Dim1 repositions in the transition from an earlier cytoplasmic pre-40S intermediate (red, Dim1 fit into EMD-4218[13]) to 80S-like ribosomes. **c.** Dim1 moves with h24 away from the platform. **d.** After repositioning the mutated FRK amino acids of Dim1 (blue) make contact with h24. Left view is similar to that in Figure 1a with the 60S subunit on the top and pre-40S on the bottom. Right view is rotated to the right by 90°. **e.** Dim1-FRK is inviable. A galactose-inducible, glucose repressible Dim1 strain (Gal::Dim1) was used to test viability. Further, mutation of Phe231, Arg233, and Lys234 (Dim1-FRK) blocks subunit joining. Whole cell extracts from cells depleted of endogenous Dim1 and Fap7 (Gal::Dim1;Gal::Fap7) and supplemented with plasmids encoding wild type or mutant Dim1 as indicated were fractionated on 10-50% sucrose gradients and the sedimentation of pre-40S ribosomes containing 20S rRNA probed by Northern blotting. 80S-like ribosomes sediment in fractions 6-7 and contain 20S and 25S rRNA. Blocking the formation of 80S-like ribosomes will lead to sedimentation of pre-40S (without 25S rRNA) in fractions 3-5[4,6,40].

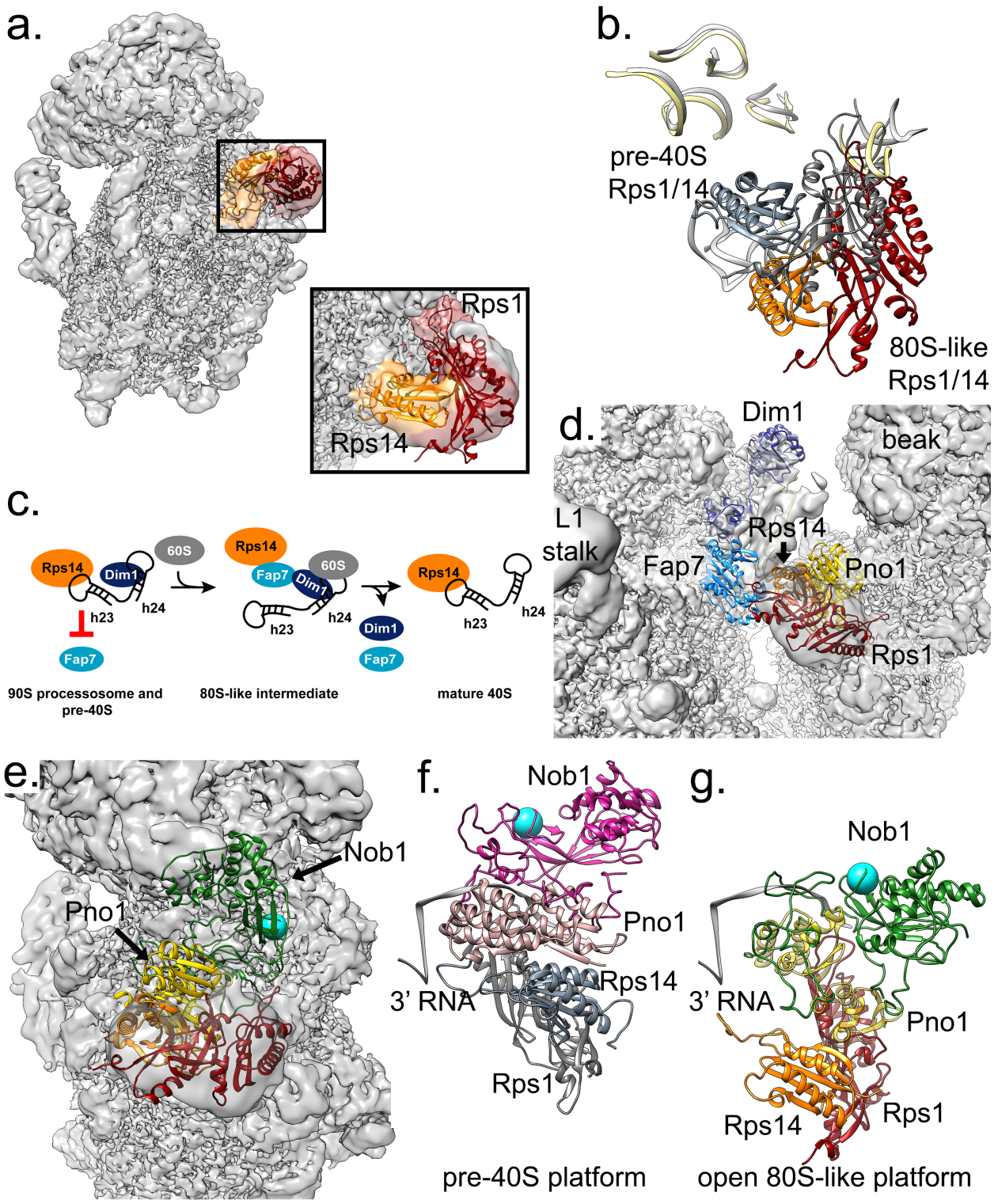
a.
Rps1
Rps14
b.
pre-40S
Rps1/14
80S-like
Rps1/14
c.
Rps14
Dim1
60S
h23
h24
Fap7
90S processosome and
pre-40S
Rps14
Fap7
Dim1
60S
h23
h24
80S-like intermediate
Dim1
Fap7
Rps14
h23
h24
mature 40S
d.
Dim1
beak
L1
stalk
Rps14
Fap7
Pno1
Rps1
e.
Nob1
Pno1
f.
Nob1
Pno1
Rps14
3' RNA
Rps1
pre-40S platform
g.
Nob1
3' RNA
Pno1
Rps14
Rps1
open 80S-like platform

Figure 4: The pre-40S platform is opened to allow for Fap7 recruitment and Nob1 repositioning. a. After local classification at the platform, alignment, and local B-factor sharpening in Relion3.0, the dominant class has density that corresponds to Rps1 (red) and Rps14 (orange), albeit not at its final position. Inset, Rps1 and Rps14 form a horseshoe-shaped dimer that fits as a rigid body in this platform density. **b.** In 80S-like ribosomes Rps1 (red) and Rps14 (orange) are shifted outwards relative to their positions in an earlier pre-40S intermediate (PDB ID 6FAI[13], Rps1, Rps14, rRNA all in gray). rRNA in 80S-like ribosomes is shown in yellow. **c.** Model for the temporal regulation of Fap7 recruitment and activity. The Fap7 binding site on Rps14 is blocked by h23 in nucleolar 90S processosomes[7-9], and earlier 40S assembly intermediates[11,13]. Opening of the platform temporarily removes h23, enabling Fap7 recruitment to promote Dim1 release[6]. **d.** Docking Fap7•Rps14 from PDB ID 4CW7[26] onto Rps14 (orange) in 80S-like ribosomes places Fap7 (cyan) in direct contact with Dim1 (blue), as predicted by previous biochemical data[6]. **e**. Superimposition of Pno1•Nob1•Rps1•Rps14 from the human pre-40S[10] places Pno1 (yellow) and Nob1 (green) so they fall in the space left by the opened platform. **f.** Nob1 in the human pre-40S structure is 30 Å and 90° away from the rRNA 3'-end (from PDB ID 6G18[10]). **g.** Repositioning of Rps1 (red) and Rps14 (orange) in 80S-like ribosomes moves Pno1 (yellow) and Nob1 (green) so that the Nob1 active site (marked by the Zn ion in space filling cyan) to be directly over the rRNA 3'-end (grey).